Finanziato dall'Unione europea NextGenerationEU

Ministero dell'Università e della Ricerca

Italiadomani PIANO NAZIONALE DI RIPRESA E RESILIENZA

NQSTI National Quantum Science and Technology Institute

Development of transmon qubits for quantum sensing and computing

Andrea Giachero

University of Milano-Bicocca

INFN - Milano-Bicocca

Bicocca Quantum Technologies (BiQuTe) Centre

6.3 **Integration of electronic devices:**

6.3.1 **Superconducting quantum gates:**

6.3.1.1 **Development of high fidelity universal quantum gates with coupled improved coherence superconducting qubits**

M12 **Design of a transmon qubit circuit with feedline and readout resonator** (2023) ✓ ☺

M24 **Fabrication and characterization of transmon qubit circuit with standard aluminum (Al) technology** (2024)
in progress ☺

M36 **Fabrication and characterization of transmon qubit circuit with improved materials for high fidelity quantum gates** (2025)

Activities in synergy with INFN's Qub-IT projects and with ICSC

Involved Groups

Fondazione Bruno Kessler
- Material study
- Fabrication
- Characterization

INFN Laboratori Nazionali di Frascati
- Theoretical computation*
- Design*
- Characterization

Università di Milano-Bicocca
- Design*
- Simulation*
- Characterization

** in collaboration with the INFN Firenze group, affiliated to Spoke 1*

Quantum Computing

- High-fidelity single- and two-qubit gates are essential building blocks for a fault-tolerant quantum computer;
- Two-qubit gates are formed by coupling together single qubits by using an intermediate electrical coupling circuit (*coupler*);
- Couplers can be implemented as fixed (resonators), tunable (dc-squid, qubit) or parametric (dc-squid) elements;

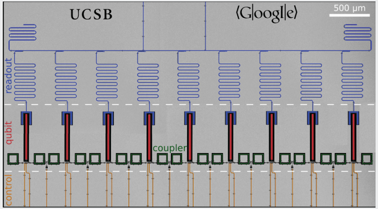

Science 360, 195-199 (2018)

Quantum Sensing

- Single qubit weakly coupled to a high-quality factor cavity can serves as photon storage/detector;
- When photons enter the storage cavity, the qubit undergoes a state change $\Rightarrow$ QND techniques allows for detecting the presence of photons in the cavity without destroying the photon status;
- By utilizing entanglement in a multi-qubit system may lead to overall improved sensitivity;

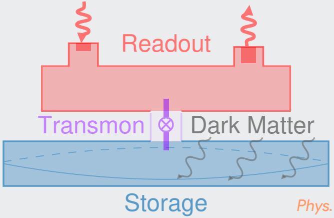

Phys. Rev. Lett. 126, 141302 (2021)

- **Transmon qubit** has become the most widely used superconducting qubit *Nature 549, 242–246 (2017)*
  - transmon regime: $E_J/E_C \sim \mathcal{O}(100)$
    E_J: Josephson energy
    E_C: charging energy
  - less sensitive to higher-order effects of the 1/f charge noise;
  - less sensitive to the problem of quasiparticle poisoning;
- **Transmon in Xmon form** *Nature 508, 500–503 (2014)*
  - straightforward connectivity: its four arms allow connections with separate elements.
    - resonator for readout;
    - control to excite the qubit state;
    - control to tune the qubit frequency;
    - quantum bus resonator
  - fast control: separate control line *Phys. Rev. Lett. 111, 080502*
  - long coherence: $T_2 \simeq 500\ \mu s$ *npj Quantum Inf 8, 3 (2022)*

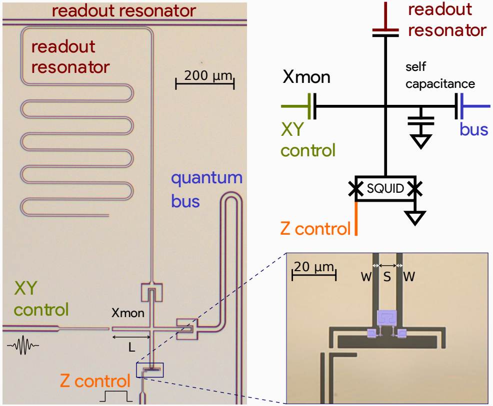

Phys. Rev. Lett. 111, 080502

$$E_C = \frac{4e^2}{2C}\ , \quad E_J = \frac{\hbar I_c}{2e}$$

Single qubit design and simulations

- **Grounded xmon transmon** *arXiv:2310.05238 [quant-ph]*
  - transmission/readout line (feedline) through a $\lambda/4$ resonator;
  - driveline to enable faster qubit control;
  - flux-bias line to tune the energy spacing between the qubit excitation levels;
- **Qubit design** created by using qiskit-metal (IBM)
  - target Hamiltonian definition;
  - qubit lines and geometry definition;
- **Electromagnetic Simulations** with commercial tools
  - Ansys HFSS for performing the eigenmode simulation and to compute the resonant frequencies;
  - Ansys Q3D for extracting capacitances and inductances;
- **Quantization** by using dedicated software packages:
  - EPR (Energy Participation ratio) + HFSS *npj Quantum Inf 7, 131 (2021)*
  - LOM (Lumped Oscillator Model) + Q3D *arXiv:2103.10344 [quant-ph]*

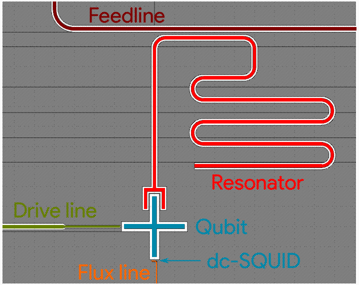

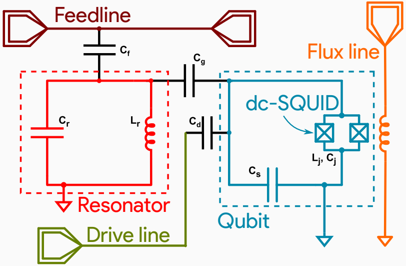

Energy Participation Ratio (EPR)

- HFSS Computes EM fields with Finite Element;
- System's eigenmodes, their frequency and the energy stored in each element per mode *m*;
- The EPR analysis computes the system eigenmodes $|\psi_m\rangle$ with $m \in$ {qubit, resonator} and computes the energy participation ratio:

$$p_m = \frac{\text{Inductive energy in JJ}}{\text{Inductive energy stored in mode m}}$$

- Kerr coefficients:

$$\chi_{nm} = \frac{\hbar\,\omega_m\,\omega_n}{4E_J} p_m\,p_n$$

- Anharmonicities: $\alpha_m = \chi_{mm}/2$
- Dispersive shifts: χ_{nm} for $n \neq m$.

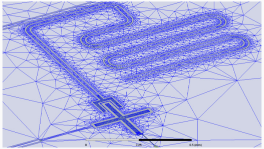

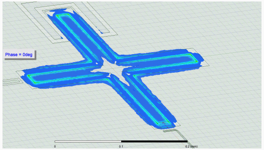

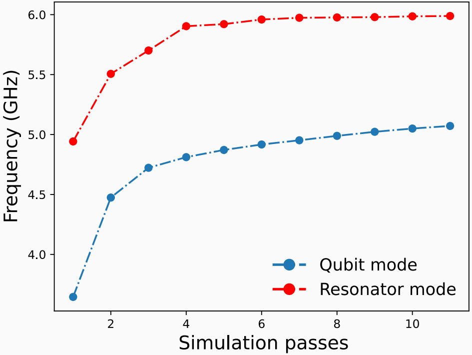

- The method builds on the quantization of lumped elements model;
- The physical layout of the quantum device is systematically partitioned into disjoint cells;
- Each cell can be independently simulated to extract its electromagnetic parameters;
- Taking a subsystem coupled to K neighbors as an example, the Hamiltonian of the composite system:

$$\hat{H}_{full} = \hat{H}_0 + \sum_{n=1}^{K} \hat{H}_n + \sum_{n=0}^{K-1} \sum_{m=n+1}^{K} \hat{H}_{nm}$$

$$\text{with} \quad \hat{H}_{nm} = \frac{\hat{Q}_n \hat{Q}_m}{C^{eff}_{nm}} + \frac{\hat{\Phi}_n \hat{\Phi}_m}{L^{eff}_{nm}}$$

where Q, Φ, L and C are extrapolated with Ansys Q3D

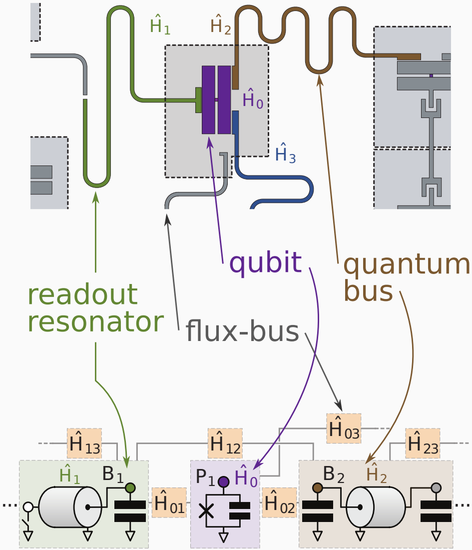

EPR vs LOM comparison

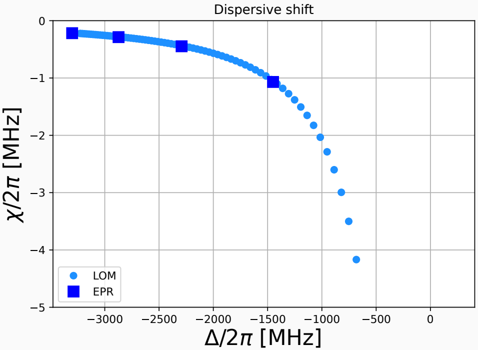

	Target	LOM	EPR
JJ Inductance L_J [nH]	10	10	10
Transmon regime E_j/E_c	>50	78.61	79.96
Anharmonicity $\alpha/2\pi$ [MHz]	202	230.62	216.44
Dispersive shift $\chi/2\pi$ [MHz]	0.30	0.31	0.35
Qubit frequency $\omega_q/2\pi$ [MHz]	5000	4995.79	4893.84
Cavity frequency $\omega_r/2\pi$ [MHz]	7400	7481.04	7435.44
Qubit-res coupling C_g [fF]	4	3.93	–

Estimated relaxation time

$Q_c \sim 4000$ and $Q_i \gtrsim 10^6 \Rightarrow T_1 \sim 70\ \mu s$

J. Appl. Phys. 104, 113904 (2008)

- Simulation results obtained at different SQUID flux-biases varying $\Delta = \omega_q - \omega_r$;
- Both EPR and LOM analyses are consistent with theory;
- Agreement between EPR and LOM for every parameter of interest within the expected margins.

- Production foreseen in 2024 at FBK after the tuning of the fabrication processes (see Felix Ahrens's talk;)
- Demonstrative two-qubit (not coupled) chip fabricated at NIST (Superconductive Electronics Group):
  - one fixed-frequency resonator driven transmon (qubit #1);
  - one tunable-frequency transmon with dedicated drive-line (qubit #2);
- Fabrication
  - Substrate: 380 nm high-resistive silicon;
  - Metal: 100 nm Niobium;
  - Junctions: Al-AlOx-Al;
  - Niobium etched also in the JJ area;
- Main goals
  - Validate and calibrate the design and simulation steps;
  - Benchmark for upcoming fabrications in Italy (CNR-IFN, FBK)

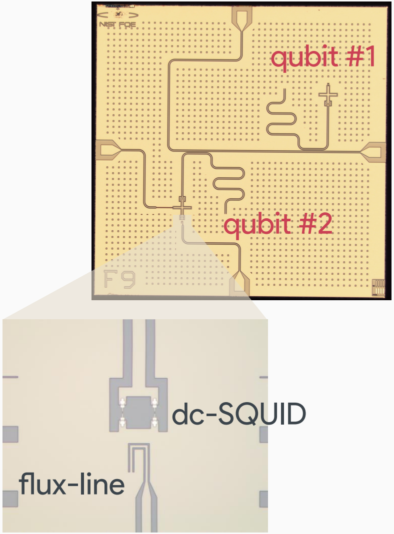

Qubit spectroscopy is performed by sweeping the frequency of the signal applied to the qubit and measuring the signal transmitted through the readout resonator;

Fixed-frequency qubit

	Measured	LOM
f_{01} [GHz]	5.689	5.682
$f_{02}/2$ [GHz]	5.589	5.579
f_{12} [GHz]	5.48 5	5.476
$f_{01} - f_{12} = \alpha/2\pi$ [MHz]	204	206
L_J [nH]	7.641	7.2

Simulations and measurements are in good agreement

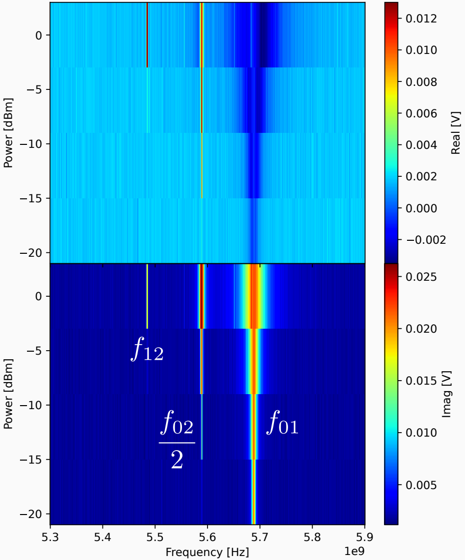

Qubit#2 spectroscopy

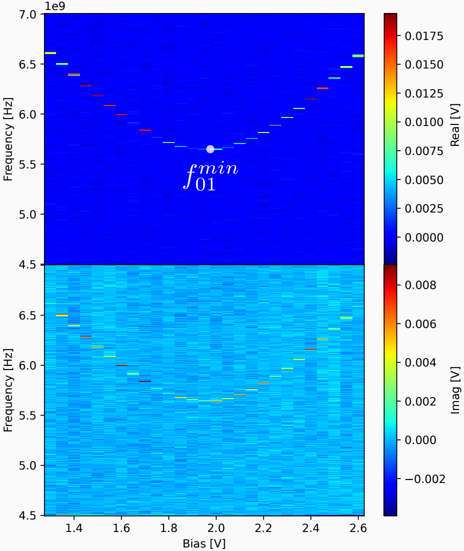

Tunable-frequency qubit

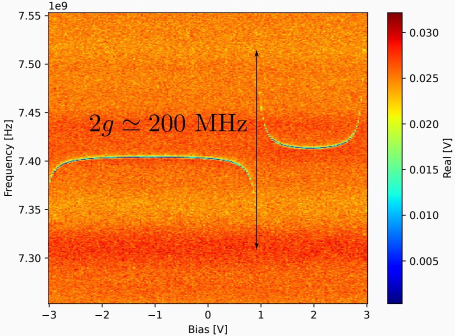

	Measured	LOM
L_J [nH]	8.364	7.9
f_{01}^{min} [GHz]	5.649	5.649
g [MHz]	98	100

Simulations and measurements are in good agreement

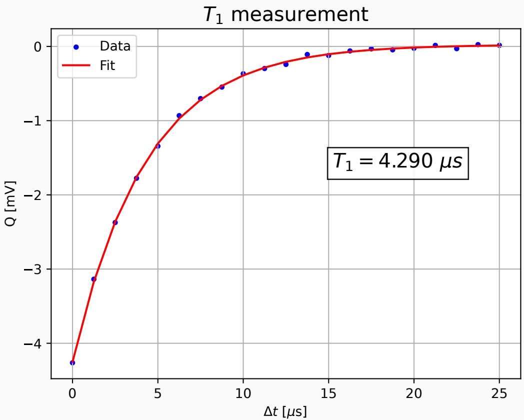

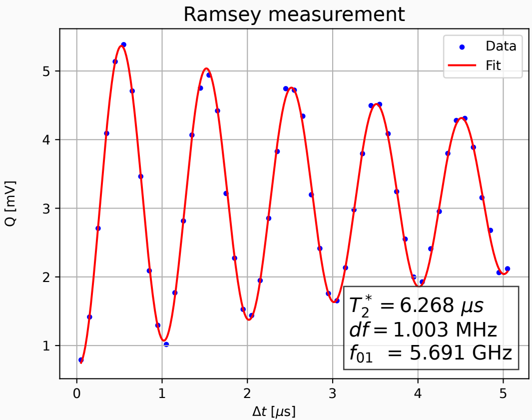

- Decoherence times one order of magnitude lower than the one estimated with simulations

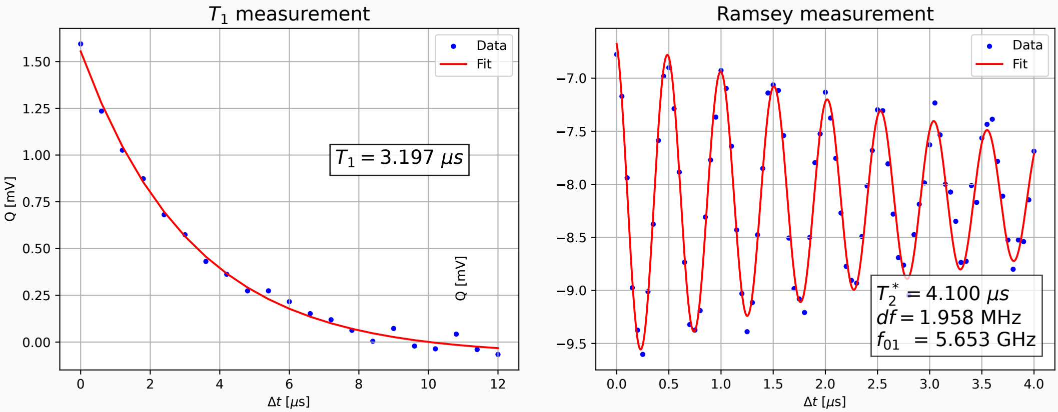

- Decoherence times one order of magnitude lower than the ones estimated with simulations;
- Decoherence times compatible with the ones measured for qubit #1;
- Design issue (less likely) or Fabrication issue (more likely);

Fixed-frequency qubit

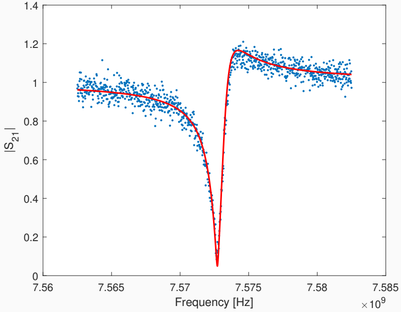

f_{res} [GHz]	7.573
Q_i	$5.624 \cdot 10^4$
Q_c	$5.063 \cdot 10^3$

Tunable-frequency qubit

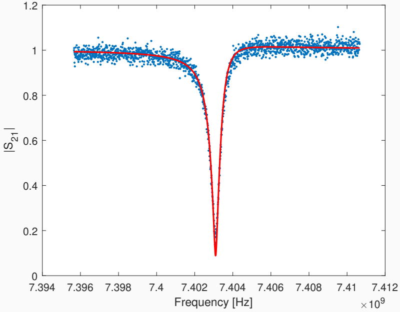

f_{res} [GHz]	7.403
Q_i	$4.027 \cdot 10^4$
Q_c	$9.673 \cdot 10^3$

- With $L_j \sim 7$ nH the expected T_1 from Purcell effect is around 24 μs $\Rightarrow$ low T_1 related to low Q_i (i.e high loss);
- Suspected fabrication issue $\Rightarrow$ different designs in the same wafer showed the same issue;
- New production for double check;

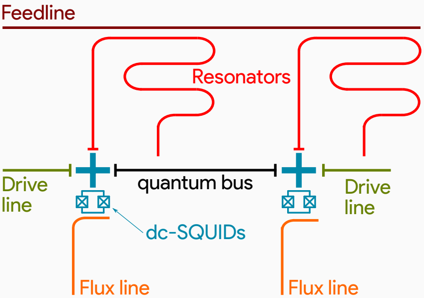

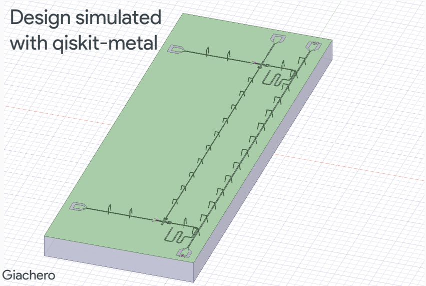

- Two Xmon qubits coupled via a cavity bus *Nature 449, 443–447 (2007)*
- Readout resonators capacitively connected at the same transmission line;
- The readout resonators are set around 8 GHz;
- Frequency of the bus resonator set to 5.5 GHz;
- The qubits are flux tunable;
- The main qubits parameters are identical;

Preliminary parameters from Q3D simulations:

Junction inductance L_j [nH]	10
Critical current I_c [nA]	32
Bus resonator capacitance C_R [fF]	368
Qubit shunt C_S [fF]	84
Quantum bus coupling C_c [fF]	1.9
Resonator coupling C_g [fF]	4.6

- A single Xmon qubit design has been simulated and developed during 2023;
- Preliminary fabrication performed at NIST;
- All predicted frequencies and couplings are close to the measured ones;
- Simulations and measurements are in good agreement;
- New wafer production will be done to confirm low T_1 and Q_i was due to fabrication and not design issue;
- New measurement scheduled in 2024 at Unimib, LNF and FBK cryogenics laboratories;
- Same design was adapted for FBK fabrication and produced soon;
- Coupled qubits design is under development

FBK/Trento group
F. Ahrens, N. Crescini, P. Falferi, F. Mantegazzini, B. Margesin, R .Mezzena, A. Vinante

LNF group
M. Beretta, F. Chiarello, A. D'Elia, D. Di Gioacchino, C. Gatti, C. Ligi, G. Maccarrone, F. Mattioli, A. S. Piedjou Komnang, L. Piersanti, A. Rettaroli, S. Tocci

Unimib group
M. Borghesi, P. Campana, R. Carobene, S. Cecchi, M. Faverzani, E. Ferri, A. Giachero, M. Gobbo, A. Irace, D. Labranca, R. Moretti, A. Nucciotti, L. Origo, S. Sanguinetti, S. Vichi

Florence group
L. Banchi, A. Cidronali, H. A. Corti

NIST group
S. Benz. J. Bieseker, M. Castellanos, P. Hopkins, D. Labranca, D. Olaya, A. Sirois